

MECHANICAL PROPERTIES OF GFR-POLYURETHANE AND -EPOXY FOR IMPACT-RESISTANT APPLICATIONS UNDER SERVICE-RELEVANT TEMPERATURES

Daniel Huelsbusch¹, Yves Mueller², Gion A. Barandun², Michael Niedermeier³ and Frank Walther¹

¹Institute for Design and Materials Testing, Department of Materials Test Engineering, TU Dortmund University, Baroper Str. 303, D-44227 Dortmund, Germany

Email: daniel.huelsbusch@tu-dortmund.de, Web Page: <http://www.wpt-info.de>

²Institute for Materials Technology and Plastics Processing, University of Applied Sciences Rapperswil, Oberseestr. 10, CH-8640 Rapperswil, Switzerland

Email: gionandrea.barandun@hsr.ch, Web Page: <http://www.iwk.hsr.ch>

³Lightweight Design and Composites Lab, University of Applied Sciences Ravensburg-Weingarten, Doggenriedstr., D-88216 Weingarten, Germany

Email: niedermeier@hs-weingarten.de, Web Page: <http://www.hs-weingarten.de>

Keywords: GFRP, impact resistance, measurement techniques, polyurethane, tempering

Abstract

Glass fibre reinforced polymers (GFRP) are increasingly gaining importance in the aircraft industry as there are great efforts to optimize the resource-efficiency. In this context GFR-Epoxy (EP) has already been implemented in a wide range of constructions. Although GFR-Polyurethane (PU) shows advantages for the use in impact-resistant applications, e.g. aerospace nose cone, the mechanical properties have not been sufficiently investigated yet. This paper presents the mechanical properties of GFR-PU compared to GFR-EP with similar layer setup. Furthermore, the processes of tempering have been investigated regarding their influence on tensile strength, compression strength after impact (CAI) and interlaminar shear strength (ILSS) under aerospace service conditions (-30°C, RT, 70°C). New fatigue test method has been used for the time- and cost-efficient estimation of the fatigue strength. High-frequency impulse measurements and digital image correlation have been applied in order to determine the deformation and damage processes. It could be shown that the use of PU increases the tensile strength of composites. Additionally, the delamination area has been reduced up to 50 % in CAI tests. Moreover, the processes of tempering improve the mechanical properties significantly, whereas an increase of temperature leads to worsened tensile and interlaminar shear strength.

1. Introduction

The aerospace industry presently is driven by optimized lightweight constructions as there is an increasing demand on resource-efficiency in terms of fuel-efficiency and sustainability. As a result fibre-reinforced polymers (FRP) proportion in airplanes increased significantly in the last years, e.g. Airbus A 350 XWB 53 % and Boeing B787 50 % [1]. Relevant advantages of FRP are based on its multi-component structure, which can be optimized regarding the specific requirements, since the combination of fibre and matrix materials provides a synergistic effect on the overall material properties, which makes composites tailorable [2]. In this context Epoxy (EP) as a resin, nowadays, is mostly used in the aerospace industry and has therefore been investigated by a number of researchers. However, Polyurethane (PU) shows advantages in terms of impact strength and abrasion compared to EP, which are of great importance for a lot of aerospace applications, e.g. aircraft nose cone. Although

GFR-PU shows great potential for aerospace applications, the mechanical properties have not been sufficiently investigated and standardized yet.

Regarding the manufacturing process of aerospace structures, most of them manufactured in time consuming prepreg-autoclave or tape-laying processes, are limited in process integration and product quantity. Furthermore, prepreg processes are costlier in energy resources compared to Resin Transfer Molding (RTM). RTM shows therefore various advantages and is a well-established manufacturing process, which is also compatible with PU. The high reactivity of PU resin compared to EP allows faster process to reduce cost and time efforts. Additionally, for thicker PU composite parts, the lower exothermic reduces the risk of local overheating due to cross-linking.

The current research focus is the characterization of GFR-PU manufactured in a High-Pressure(HP)-RTM process with variation of post heat-treatment processes. The mechanical properties of GFR-PU are investigated with a combined measurement setup to determine the damage and deformation behaviour and compared to existing GFR-EP from the aerospace industry.

2. Manufacturing of GFR-Polyurethane

A HP-RTM process has been developed to manufacture GFR-PU plates. The resin properties of PU and EP are displayed in Table 1. A high pressure mixing machine (Isotherm PSM90) with a self-cleaning mixing head (GP600) has been applied to the HP-RTM system. The dry preform is made out of 16-layers in quasi-isotropic [45/-45/0/90/45/-45/0/90]s setup of satin weave glass fibre fabric with a density of 300 g/m² and fibre volume fraction of 46 %. The dry preform is placed in the preheated mold (85°C) and the PU resin is injected for 40 s at a resin injection rate of 7 g/s under an applied vacuum of 0.8 bar. The cavity pressure in the HP-RTM process achieved during injection up to 45 bar and the part is demolded after 5 minutes. The GFR-EP prepreg laminate was realised with the same quasi-isotropic ply orientations in a classical autoclave process. A fibre volume fraction of 46 % was reached. The test specimens were machined from the GFRP plates by water cutting after post-curing in a furnace (Nabertherm TR450) at 120°C for 7 hours, whereas a temper cycle of 4 hours is sufficient to improve the mechanical properties at high temperature. The specimen geometries were defined according to standards DIN527-4 (Type 1B) and DIN 14130-1.

Table 1. Neat resin properties.

	<i>PU</i>	<i>EP</i>
Young's modulus (GPa)	3.1	3.9
Tensile strength (MPa)	62.8	47.7
Fracture strain (10 ⁻²)	9.1	1.5
Glass transition T _g (°C)	130 (DSC)	190 (DMTA)

For qualitative assessment of the consolidation processes of the two materials, materialographic investigations of the GFRP laminates were carried out using scanning electron microscope (Tescan Mira-3). Therefore materialographic sections were prepared from source material and sputtered with gold.

In Fig. 1 it can be seen that both GFR-EP and GFR-PU exhibit great fibre impregnation, as there are no unbonded fibre-matrix areas. Figure 1a displays the materialographic section of GFR-EP, which indicates high layer quality due to no evident flaws in the matrix structure. Instead, the parts of GFR-PU show several voids in the materialographic section. The reasons for this could be non-ideal clamping preform in the mold or outgassing resin until demolding. In following research, the process will be optimized by using thermoplastic powdered fabric to prevent fibre washing and voids.

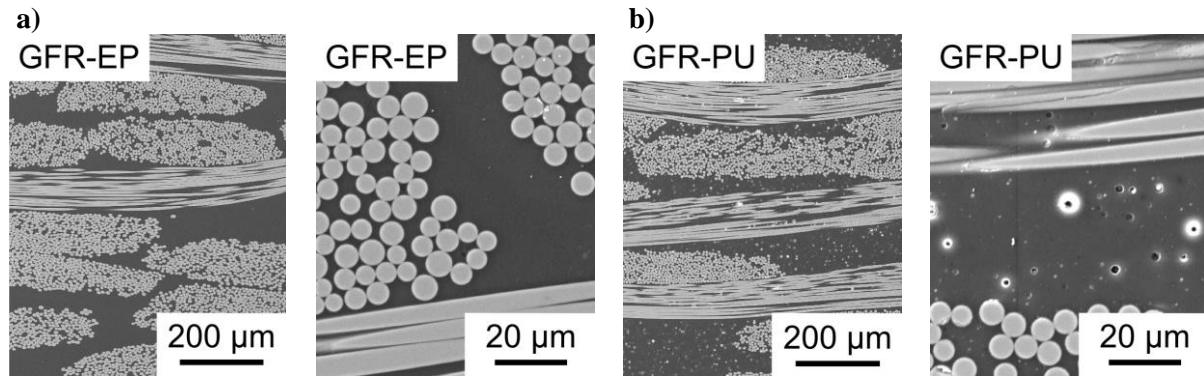


Figure 1. Micrographs of the longitudinal section of (a) GFR-EP and (b) GFR-PU

3. Testing Strategy and Experimental Setup

3.1. Quasi-Static Investigations

Quasi-static tensile tests were carried out at universal testing system (Shimadzu, AG-X Plus, $F_{\max} = 100$ kN) in accordance to DIN527-4 at a displacement rate of 2 mm/min equivalent to a strain rate of $6.7 \cdot 10^{-4} \text{ s}^{-1}$. Strain measurements were performed using 3D-digital image correlation (DIC) (Limes, Q400) to determine the local strain in order to localize damages. High-frequency impulse measurements (HFIM) (Qass, Optimizer 4D) were utilized to detect structure-borne sound with the objectives of monitoring the damage development as well as to separate the damage mechanisms.

Investigations of the interlaminar shear strength (ILSS) were performed at universal testing system (Instron, 5567, $F_{\max} = 30$ kN) with respect to DIN 14130-1 at a displacement rate of 1 mm/min. The interlaminar shear strength for each specimen was calculated with respect to DIN 14130-1 as shown in the following equation:

$$ILSS = \sqrt[3]{4} \cdot F_{\max,ILSS} / A \quad (1)$$

The compression strength after impact (CAI) has been determined based on the standard ASTM D7136. The defect-free and ultrasonic-scanned plates were first damaged with a drop tower (IWK, in-house development) of 30 J impact energy. The delamination area for each specimen was measured with an ultrasonic device (Olympus, Omniscan-MX2). The compression strength was determined with a universal testing system (Shimadzu, AG-X, $F_{\max} = 250$ kN), a compression test tool and a displacement rate of 0.5 mm/min according to ASTM D7136.

To determine the quasi-static mechanical properties under service-relevant temperatures for aerospace industry and to ensure constant testing conditions, the tests were carried out in climate chambers at constant temperatures (-30°C, 70°C).

3.2. Cyclic Investigations

For the investigation of the fatigue behaviour, instrumented multiple step tests (MST) were performed at servo-hydraulic testing system (Instron, 8801, $F_{\max} = \pm 100$ kN) with the stress ratio $R = 0.1$ and the frequency 7 Hz using sinusoidal load-time function at room temperature. MST exhibit the opportunity of resource-efficient estimation of the fatigue properties of various materials and has been successfully applied for FRP in previous studies [3, 4]. The maximum stress amplitude σ_{\max} is increased stepwise from $\sigma_{\max,start} = 20$ MPa after $\Delta N = 10^4$ cycles by $\Delta \sigma_{\max} = 20$ MPa until failure. For estimation of the fatigue properties, the material response is determined in terms of measuring total strain amplitude $\varepsilon_{a,t}$.

total mean strain $\epsilon_{m,t}$, dynamic modulus E_{dyn} and change in temperature ΔT_{max} , which are displayed as cycle- and load-dependent functions. For strain measurements a mechanical extensometer was applied (Instron, $l_0 = 50$ mm, $\Delta l = \pm 5$ mm). The temperature was measured with thermocouples at three positions on specimen surface as well as a reference temperature representing room temperature. The change in temperature was calculated by the maximum difference of surface to reference temperature. The damage development can be estimated by the change of the measurand values, whereas the failure stress $\sigma_{max,f}$ can be determined as the maximum stress level in the MST.

4. Results and Discussion

4.1. Quasi-Static Investigations

The stress-strain curves of the tensile tests for each material are depicted in Fig. 2a and b. The curves for GFR-PU show a nearly linear slope until fracture, whereas GFR-EP presents a pronounced bend at approx. 0.7 % total strain. Furthermore, GFR-EP exhibits higher stiffness and less tensile strength compared to GFR-PU. Fig. 2c shows exemplary the results of HFIM. When damage occurs in a composite, it leads to acoustic emissions due to rapidly released elastic energy [5]. The detected acoustic emissions are displayed in a process landscape after Fast Fourier Transformation (FFT).

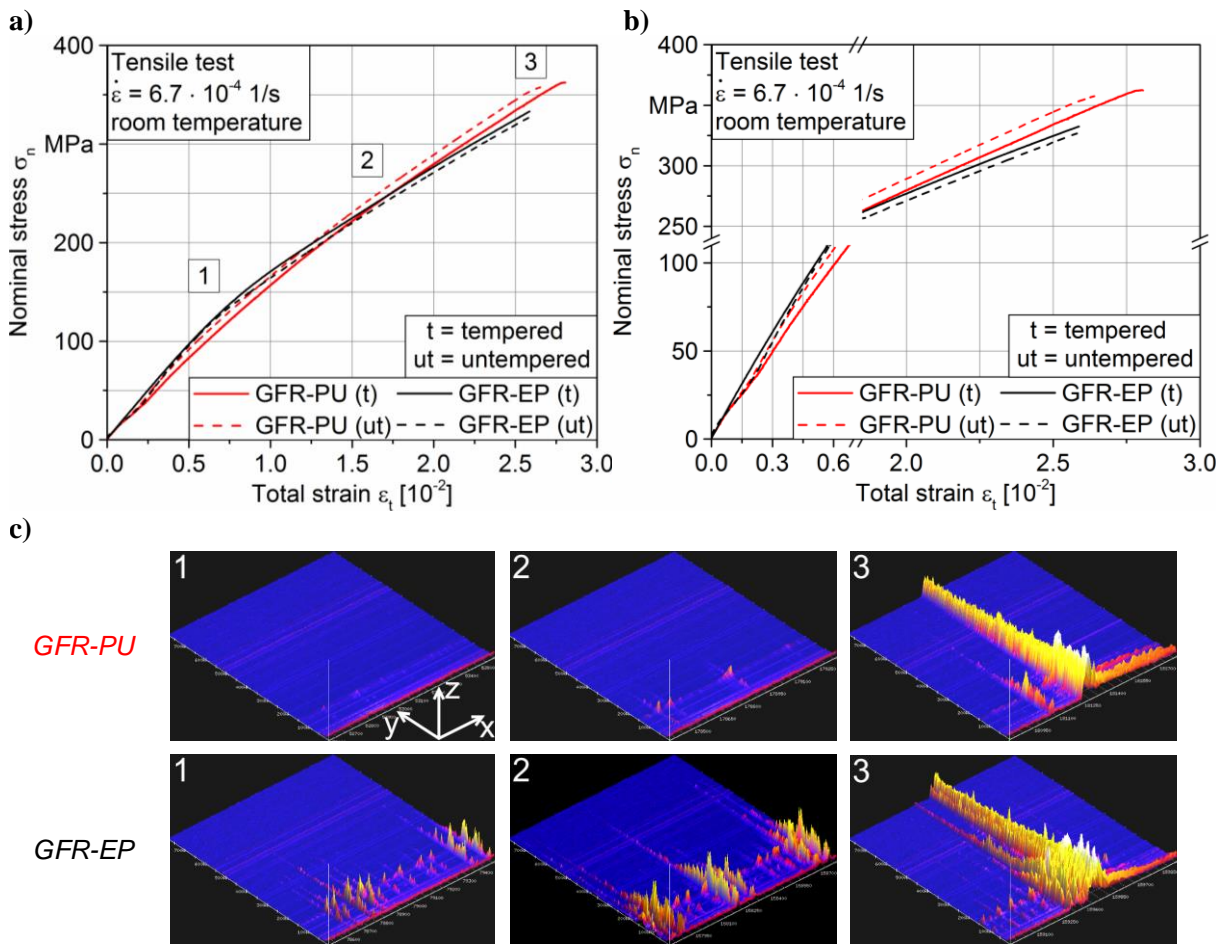


Figure 2. Tensile tests: (a) Stress-strain diagram and (b) details from 0.0 to 0.7 and 1.9 to $3.0 \cdot 10^{-2}$ total strain; (c) acoustic emissions; for GFR-PU and GFR-EP

The energy amplitude (z-axis) is plotted time discrete (x-axis) as a function of frequency (y-axis). In addition, energy amplitude and frequency spectrum indicate the damage mechanisms in terms of fibre breaking, fibre-matrix debonding and delamination [6]. However, it can be seen that tensile loading on GFR-PU doesn't result in relevant acoustic emissions until fracture (Fig. 2c-3), which represents a high layer quality and great fibre-matrix interface. In contrast, tensile loading of GFR-EP causes various acoustic emissions. The detected signals in Fig. 2c-1 and -2 show smaller frequency spectrums and less energy amplitude as the signals detected at fracture in Fig.2c-3. This indicates occurrence of different damage mechanisms, e.g. fibre-matrix debonding or delamination. However, the damage development in GFR-EP can be a reason for the stiffness degradation in tensile tests after approx. 0.7 % total strain.

The numerical results for tensile strength and fracture strain at service-relevant temperatures are summarized in Table 2. It is obvious that tempering leads to a significant increase of tensile strength at high temperature (70°C) for GFR-PU. In contrast, the relative decrease of tensile strength for untempered GFR-PU from -30°C to 70°C is higher compared to untempered GFR-EP, which can be explained by less glass transition temperature (T_g) of PU (Table 1). For GFR-EP, the temper cycle has no influence on tensile properties at high temperature. At room temperature the influence of tempering is neither for GFR-PU nor GFR-EP perceptible, anyhow PU shows better performance.

Table 2. Results of tensile tests at service-relevant temperatures, for tempered (t) and untempered (ut) GFR-PU and GFR-EP.

	Temperature	<i>GFR-PU</i> (t)	<i>GFR-PU</i> (ut)	<i>GFR-EP</i> (t)	<i>GFR-EP</i> (ut)
Tensile strength (MPa)	-30°C	389.3	366.7	406.7	373.0
	RT	346.3	343.3	333.6	329.6
	70°C	313.2	270.0	297.4	295.5
Fracture strain (10 ⁻²)	-30°C	-	-	-	-
	RT	2.67	2.66	2.49	2.73
	70°C	2.46	2.28	2.22	2.51

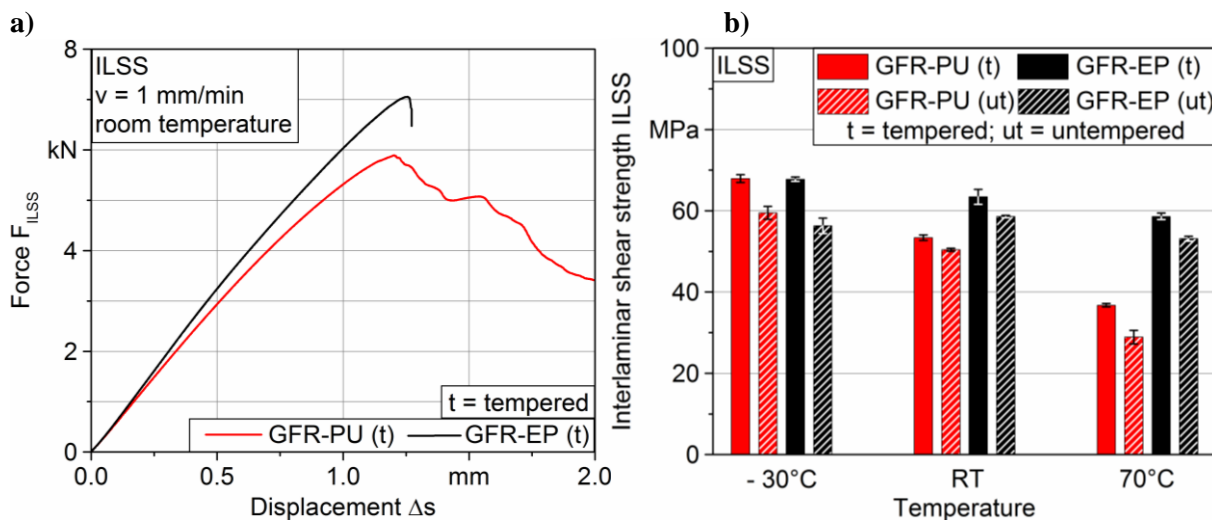


Figure 3. Interlaminar shear strength (ILSS) tests: (a) Force-displacement diagram at room temperature and (b) interlaminar shear strengths at service-relevant temperatures; for GFR-PU and GFR-EP.

Results of interlaminar shear strength tests are exemplary displayed in terms of force as a function of displacement for GFR-PU compared to GFR-EP in tempered configuration. A linear slope can be seen until maximum force for both materials, whereas GFR-PU shows a slow decrease of stiffness and GFR-EP a rapid fracture after maximum force. The different deformation behaviour can be explained by various matrix properties or an influence of manufacturing process [7]. Especially the fracture behaviour of GFR-EP seems to be due to brittle properties of EP compared to PU (Table 1). In Fig. 3b, the ILSS for each material is plotted against temperature. GFR-EP exhibits better performance compared to GFR-PU with increasing temperature due to higher T_g of EP. Another finding is that tempering leads to improved ILSS for GFR-PU especially at low and high temperatures, as it has been also identified in tensile tests. This may result out of an optimized molecule structure of the matrix and an optimized fibre-matrix interface based on the tempering process.

In Fig. 4, the results of compression strength after impact (CAI) tests are displayed. Figure 4a shows the compression strength for intact and damaged specimens. There is no numerical evidence visible for the compression strength, neither positive nor negative influences of tempering GFR-PU for intact plates. For damaged plates, the brittle behaviour leads to a higher delamination area when tempered, although the compressive strength is only slightly lower. With further Shore D hardness measurements there were no variation in surface hardness caused by temper cycle obvious. For GFR-EP higher compression strength is reached when tempered as well as a reduced delamination area after impact. Thus, in contrast to GFR-PU, the delamination area is decreasing using the temper cycle.

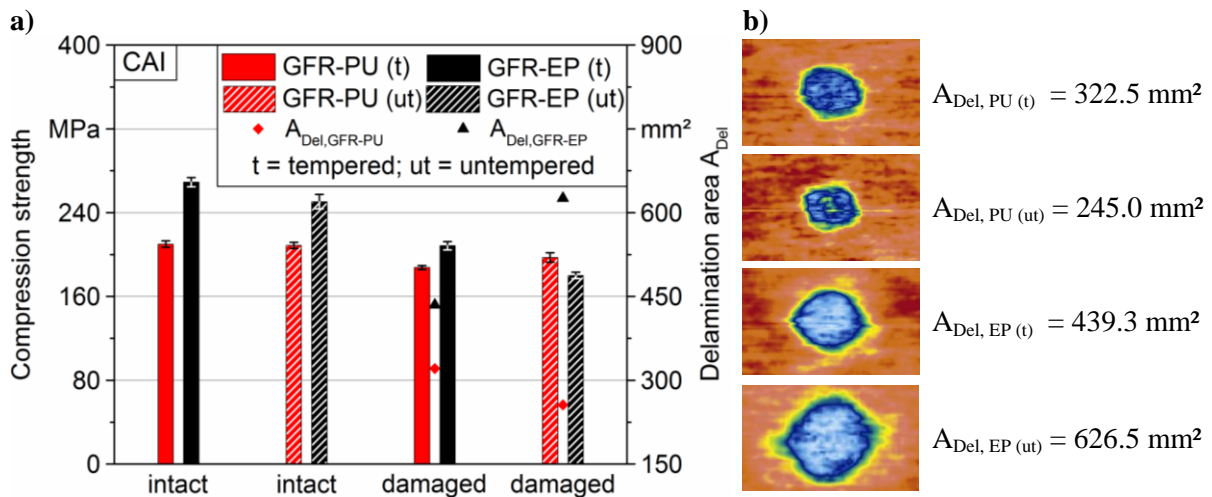


Figure 4. Compression strength after impact (CAI) tests: (a) Compression strength for intact and damaged specimens; (b) delamination areas after impact; for GFR-PU and GFR-EP.

4.2. Cyclic Investigations

Figure 5 exemplary presents a result of multiple step test (MST) for tempered GFR-PU. The black curve shows the maximum stress until failure at 180 MPa. The measurands in terms of total strain amplitude $\epsilon_{a,t}$, total mean strain $\epsilon_{m,t}$, dynamic modulus E_{dyn} and change in temperature ΔT_{max} are plotted as function of number of cycles N , respectively, as well as the maximum stress σ_{max} as the controlled value. Total strain amplitude and total mean strain are increasing stepwise depending on maximum stress development. However, a change of measurands within loading step indicates beginning damage evolution [4], which can be identified at $\sigma_{max} = 100 \text{ MPa}$. The further increase of strain values within the following steps represents a proceeding damage evolution until failure. In addition, E_{dyn} has been calculated based on hysteresis measurements as basis for stiffness degradation assessment. It can be seen that stiffness reduction corresponds to the temperature increase

qualitatively, which firstly shows a significant increase at 100 MPa. Furthermore, the stiffness degradation per step after 100 MPa shows a fast decrease at the step beginning and a slow decrease until step end, which corresponds to the behaviour of stiffness degradation of composites in constant amplitude tests [8, 9]. Since the measurement setup has a significant influence on the measured hysteresis and, therefore, on the determined stiffness, the results have to be compared and validated with DIC measurements. However, the largest relatively change in value is shown by change in temperature, which is a useful indicator for actual specimen condition. Therefore the influence of frequency on temperature development has to be numerically determined before.

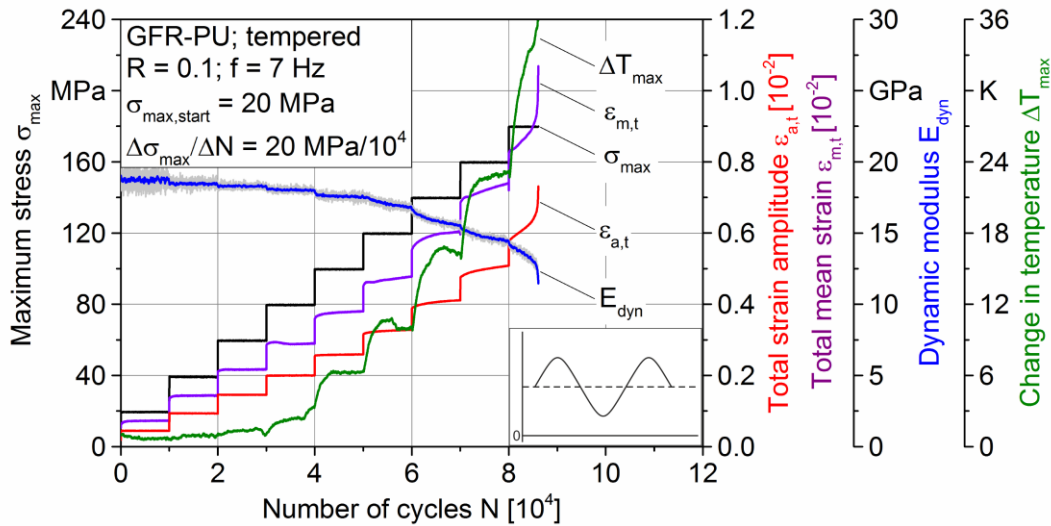


Figure 5. Results of multiple step test (MST) with tempered GFR-PU specimen.

The results for the maximum failure stress of GFR-PU and GFR-EP in multiple step tests are plotted in Tab. 3. In untempered configuration GFR-PU and -EP lead to a fatigue strength of 200 MPa. Furthermore, tempering leads to a negative influence on the fatigue strength of GFR-PU, whereby the fatigue strength of GFR-EP increases as expected. The poor results of GFR-PU in multiple step tests compared to tensile tests may be a result of voids (Fig. 1b), which seem to have an important influence on the results under fatigue loading, since damage may occur in the subsurface.

Table 3. Maximum failure stress in multiple step tests, for tempered (t) and untempered (ut) GFR-PU and GFR-EP.

Maximum failure stress (MPa)	<i>GFR-PU (t)</i>	<i>GFR-PU (ut)</i>	<i>GFR-EP (t)</i>	<i>GFR-EP (ut)</i>
$\sigma_{\max, f}$	180	200	220	200

5. Conclusions and Outlook

Glass fibre reinforced polyurethane (GFR-PU) manufactured in a newly developed high-pressure-(HP-) RTM process has been characterized in terms of tensile strength, interlaminar shear strength (ILSS), compression strength after impact (CAI) and fatigue strength under service-relevant temperatures. Determined mechanical properties were compared to existing glass fibre-reinforced

epoxy (GFR-EP) from aerospace industry. Furthermore, a tempering process has been applied and the influence on the mechanical properties has been investigated.

Following findings can be concluded:

1. GFR-PU shows high potential for the use in impact-resistant applications due to high tensile strength and small delamination area.
2. Tempering of GFR-PU seems to have an influence on the chemical properties and leads to an increase of strength (tensile strength/ILSS) and a decrease of ductility (delamination area).
3. Tempering processes seem to have a higher influence on GFR-PU than on GFR-EP regarding strength, especially for higher temperature fields.
4. Fatigue properties and ILSS get degraded compared to GFR-EP, which may be due to voids.
5. The developed HP-RTM process shows high potential for efficient manufacturing of GFR-PU.

In further studies, binder is going to be implemented in the manufacturing process in order to reduce void proportion and time effort. The influence of binder will be investigated and the mechanical properties will be compared to the existing results. Furthermore, the stiffness degradation of GFR-PU in fatigue tests will be combined with in-situ quasi-static tests for assessment of the damage state.

Acknowledgments

The authors thank the „Bundesministerium für Wirtschaft und Energie“ (BMWi) for the funding of this research project (code KF2198131) as well as the „Kommission für Technologie und Innovation“ (KTI) for supporting the partners from Switzerland in this EUREKA research project.

References

- [1] G. Marsh. Airbus A350 XWB update. *Reinforced Plastics*, 54, 6:20-24, 2010.
- [2] H. Estrada and L. S. Lee. FRP Composite Constituent Materials. In *The International Handbook of FRP Composites in Civil Engineering*. CRC Press Taylor & Francis Group, 31-32, 2014.
- [3] F. Walther. Microstructure-oriented fatigue assessment of construction materials and joints using short-time load increase procedure. *MP Materials Testing*, 56, 7-8:519-527, 2014.
- [4] D. Huelsbusch, M. Haack, A. Solbach, C. Emmelmann and F. Walther. Influence of pin size on tensile and fatigue behaviour of Ti-CFRP hybrid structures produced by laser additive manufacturing. *Proceedings 20th Int. Conference on Composite Materials ICCM-20, Copenhagen, Denmark, July 19-24, 2015*.
- [5] V. Lopresto, C. Leone, G. Caprino and I. de Iorio. Analysis of acoustic emission signals produced by different carbon fibre reinforced plastic laminates. *Proceedings 17th Int. Conference on Composite Materials ICCM-17, Edinburgh, Scotland, July 27-31, 2009*.
- [6] S. A. Carey. Acoustic emission and acousto-ultrasonic signature analysis of failure mechanisms in carbon fiber reinforced polymer materials. *Ph.D. thesis, South Carolina, USA, 2008*.
- [7] I. Gürkan and H. Cebeci. An approach to identify complex CNT reinforcement effect on the interlaminar shear strength of prepreg composites by Taguchi method. *Composites Structures*, 141:172-178, 2016.
- [8] A. W. Wharmby, F. Ellyin and J. D. Wolodko. Observations on damage development in fibre reinforced polymer laminates under cyclic loading. *International Journal of Fatigue*, 25:437-446, 2003.
- [9] T. Peng, Y. Liu, A. Saxena and K. Goebel. In-situ fatigue life prognosis for composite laminates based on stiffness degradation. *Composite Structures*, 132:155-165, 2015.